

Enhancing methane sensors by sensing without detection

ARTHUR C. CARDOSO,^{1,*} HAICHEN ZHOU,¹ SIDDARTH K. JOSHI,¹ AND JOHN G. RARITY¹

¹*Dept. of Electrical and Electronic Engineering, University of Bristol, Merchant Venturers Building, Woodland Road, Bristol BS8 1UB, UK*

**arthur.cardoso@bristol.ac.uk*

Abstract: We propose a novel methane sensor based on sensing without detection. First used in quantum imaging, this technique relies on the interference effects seen in three wave mixing when pump signal and idler modes make a double pass through a nonlinear crystal. The method allows sensing at wavelengths where detectors are poor and detecting at wavelengths where photon counting sensitivity can be achieved. This compact interferometer, potentially set in a portable device for field operations, could allow the detection of low concentrations of methane at up to 100m range. Signal-to-noise ratio calculations point out that the method's sensitivity can overcome the integrated path differential absorption direct sensing at high non-linear gain regimes.

© 2022 Optica Publishing Group under the terms of the [Optica Publishing Group Publishing Agreement](#)

1. Introduction

Methane is the second most important greenhouse gas in the Earth's atmosphere, its global warming potential is up to eighty-four times more than carbon dioxide in a twenty years period [1, 2], providing a huge contribution to the rise of temperature and related climate change. The concentration of this gas in the atmosphere has been rising since the beginning of the industrial age, and it is caused by anthropogenic and natural sources [3–5]. Agricultural, use and extraction of fossil fuels, biomass burning and decomposition of organic matter in wastes and landfills are the most important contributions among the human CH₄ sources [6]. Thus, monitoring and control of methane emissions is crucial to reduce global warming and mitigate climate changes [7].

Over the last decades scientist have endeavoured to develop new accurate methods to measure methane concentrations in the air. Many different experiments exploring optical methane sensors were performed using spaceborne [8, 9], airborne [10, 11] and short range sensors [12, 13]. They approach miscellaneous techniques like Integrated Path Differential Absorption (IPDA), Differential Absorption Lidar (DIAL), Dual-comb spectroscopy (DCS), spectral analysis of light among others methods. Modern short range DIAL methane sensors [12, 13] are able to detect sources with high spatial and depth resolution with high sensitivity, being the state-of-art technology to identify small sources up to hundreds of meters away.

This paper proposes a novel method for short range methane sensing based on sensing without detection. Formerly exploited for imaging [14, 15], this technique makes use of high-correlated light sources in a nonlinear interferometer to collect phase and amplitude images of an object, by detecting light that never interacted with it. Recently, this methodology has been extended for several applications like spectroscopy [16], microscopy [17, 18], quantum holography [19], optical coherence tomography [20, 21] and terahertz sensing [22]. Methane exhibits a strong absorption at middle infrared (MIR) spectra, up to one hundred times greater than at short wave infrared (SWIR), but MIR light detection is quite challenging due to thermal noise background and low-efficiency detectors. Sensing without detection enables a two-colour system that is particularly useful in this case because it allows illumination of the gas at a wavelength for which

it has a high absorbance and detection at a wavelength where low-noise and efficient detectors are available.

2. Proposed experimental apparatus and signal-to-noise ratio

2.1. Proposed experimental scheme

The nonlinear interferometer proposed for methane sensing is depicted in Fig.1 and relies on high-gain light sources generated by stimulated parametric down conversion (SPDC).

A pump and an idler laser lasers are overlapped in a nonlinear crystal (NLC) stimulating the generation of a signal mode by SPDC. The signal field is short wave infrared while the idler is MIR and can be tuned onto resonance with methane absorption lines. The idler laser passed through a gas plume, hits a background, which could be a mirror or partially reflective surface, and is scattered back into the interferometer. The pump and the signal modes are reflected back to the crystal by a highly reflective mirror. In the second pass through the crystal the pump and idler mode generate a phase dependent amplification of the signal field and the resulting intensity is measured in a sensitive (ie photon counting) detector. The phase shifter (PS) can be used to adjust the phase of the idler mode to produce amplification or deamplification at the second down conversion. As a result the signal mode generated will show an interference pattern with period reflecting the idler mode wavelength.

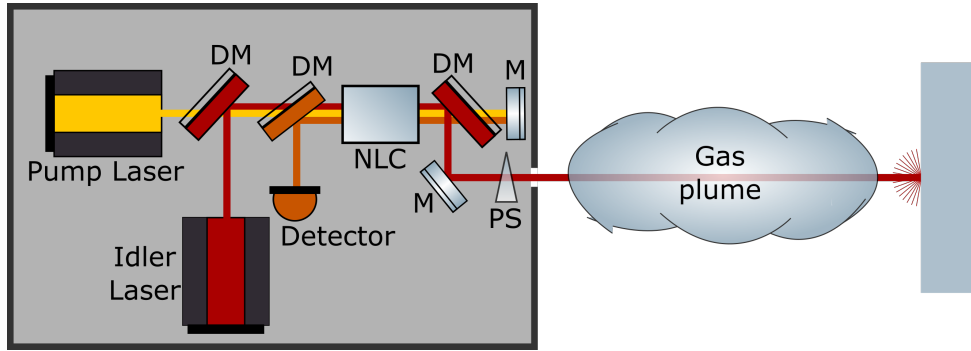


Fig. 1. Scheme proposed for gas sensing without detection. Pump and idler laser beams are combined in a dichroic mirror (DM) to overlap in a nonlinear crystal (NLC) generating a signal mode. The pump laser and the signal field are reflected back to the crystal by a highly reflective mirror (M). The idler mode is deflected by a dichroic mirror and passed through a gas plume and scattered back to the crystal from a passive Lambertian background or (partial) retroreflector. In the second interaction of the pump and idler fields with the NLC, a weak phase dependent amplification of the signal mode occurs and the resulting light is directed to a sensitive (photon counting) detector. By adjusting the idler laser's phase with the phase shifter (PS), amplification and de-amplification can be measured in the signal beam as an interference fringe. The visibility of this interference pattern contains information on the absorption of the idler beam by the gas plume

The magnitude of the modulation of the signal field is proportional to the field returning through the gas plume and hence the visibility of the interference pattern carries a measure of the absorption in the idler path. When the idler laser is tuned to a wavelength at which methane is transparent (off-resonance), we will observe a high visibility interference pattern. Otherwise, if it is tuned to spectral region where methane exhibits a high absorbance (on-resonance) we will observe a loss of visibility in the interference pattern effectively due to the interference between paths with different intensities. By comparing the visibilities of the two interference patterns, we are able to calculate out the amount of MIR light absorbed and estimate the methane concentration in the gas plume, by detecting only the signal mode that never interacted with it.

As a proof of principle, a laboratory experiment has been set up using a mirror to reflect back the idler mode. The apparatus is designed to measure methane levels in gas cells. In the experiment we use a $1.064\mu\text{m}$ laser to pump a PPLN crystal and a $3.392\mu\text{m}$ He-Ne laser to stimulate the SPDC. A single photon counting InGaAs signal detector of 2.5% nominal efficiency detects photons at $1.55\mu\text{m}$. A set of filters of around 0.6% transmittance keeps the count rate under the saturation rate of the detector. By translating the mirror that reflects the idler laser back to the crystal we change the relative phase between the modes. This enables us to measure an interference pattern, shown in Fig.2. The visibility of the fringe is $(92 \pm 3)\%$ and its period

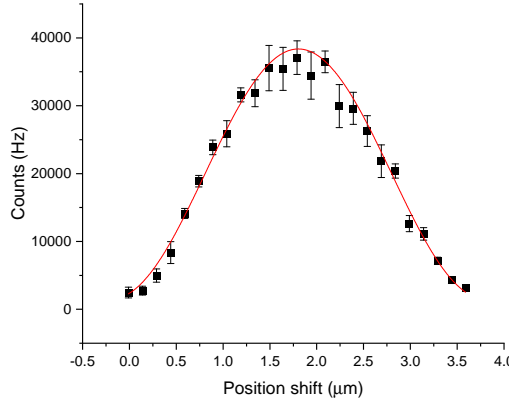


Fig. 2. Graph of the number of counts measured by the signal detector as function of the length of the increment path of the idler laser's path.

is approximately the idler laser wavelength. The next steps for the experiment is to change the stimulating laser to a tunable one and measure methane concentrations in gas cells with different methane concentrations.

2.2. Signal-to-noise ratio

The intensity of the signal mode generated by the SPDC is

$$I_s = \left(\frac{\mu_0 \epsilon_0 \chi^{(2)} \omega_s^2 L}{2k_s} \right)^2 I_p I_i, \quad (1)$$

where μ_0 is the magnetic vacuum permeability, ϵ_0 is the electric vacuum permeability, $\chi^{(2)}$ is the effective non-linearity of the nonlinear crystal, L is its length, ω_s is the angular frequency of the signal mode, k_s its wave-vector's modulus, I_p the intensity of the pump laser and I_i the intensity of the idler laser. Eq.(1) can be written as $I_s = G I_i$, where $G = \left(\frac{\mu_0 \epsilon_0 \chi^{(2)} \omega_s^2 L}{2k_s} \right)^2 I_p$ is a gain factor related to the SPDC process.

On the first pass through the crystal we create a small amount of light I_{s1} in the signal beam stimulated by the idler intensity I_i and a small amount of extra light in the idler

$$I_{s1} = G I_i, \quad I_{i1} = I_i (1 + G) \quad (2)$$

In our experiments with low intensity CW pump light $G \ll 1$ and we can ignore the any higher order (exponential) gain effects and assume no pump depletion. On returning through the crystal a second gain process occurs

$$I_{s2} = G I_i \alpha \mathcal{T}^2 \quad (3)$$

again ignoring higher order terms in G and where α is the reflectivity of the target and \mathcal{T} is the (single pass) transmission through the gas plume. However the two signal fields created are not necessarily in phase due the differences in relative paths to the mirrors for pump signal and idler. In the case where $I_{s1} \gg I_{s2}$ we can treat this interference process in same way as homodyne detection which be written as

$$I = I_{LO} + I_{s2} + 2\sqrt{I_{LO}I_{sig}} \cos \phi, \quad (4)$$

In our method (Fig.1), we identify the local oscillator as the signal mode generated by the SPDC in the first passage through the crystal $I_{LO} = I_{s1}$ and I_{s2} is the potential intensity generated on the second pass while

$$\phi = \phi_p - \phi_i - \phi_s$$

is the relative phase between the pump, and signal and idler fields.

The signal-to-noise ratio (SNR) can then be analysed in a similar way to homodyne interferometry [23]. The detected signal on- and off-resonance can be written in terms of the difference between maximum and minimum photon counts of an interference fringe received, R , and its variance, V ,

$$R = \frac{2\eta T_{int}}{\hbar\omega_s} \sqrt{\langle P_{sig} \rangle \langle P_{LO} \rangle}, \text{ and} \quad (5)$$

$$V \approx \eta T_{int} \frac{\langle P_{LO} \rangle}{\hbar\omega_s}, \quad (6)$$

where: η is the efficiency of the detector, $\hbar\omega_s$ is the energy of a signal photon $\langle P_{sig} \rangle$ is the power of the signal input, $\langle P_{LO} \rangle$ is the power of the local oscillator and T_{int} is the measurement time. For comparison with direct detection schemes we assume signal is estimated from the difference of maximum and minimum of fringe measured in time $T_{int}/2$. We considered that the system is shot-noise limited, that is, the noise produced by the photon number fluctuations is much greater than the environment and detector's noise. Also, as the noise provided by the signal is much smaller than the local oscillator's noise, we neglect it. So, the SNR on- and off-resonance can be written in terms of the number of photons combining Eq.(5) and Eq.(6) as

$$SNR_{on,off} = \frac{R_{on,off}}{\sqrt{V_{on,off}}} = 2\sqrt{\langle n_{sig} \rangle_{on,off}}, \quad (7)$$

where $\langle n_{sig} \rangle_{on}$ and $\langle n_{sig} \rangle_{off}$ are the average number of photons generated by the second SPDC in the nonlinear crystal counted by the detector at on- and off- resonance, respectively

$$\langle n_{sig} \rangle_{on,off} = \eta G \alpha \mathcal{T}_{on,off}^2 T_{int} \frac{P_i}{\hbar\omega_s}. \quad (8)$$

where α is the reflectivity of the background and \mathcal{T}_{on} and \mathcal{T}_{off} are the transmittances of the gas plume on- and off-resonance MIR idler wavelengths, and P_i the power of the idler laser. In this case, we will take the background as a Lambertian or partially retroreflecting surface. Also, as the methane lines are narrow, we considered the same gain, detector efficiency, angular frequency and stimulating laser (idler) power for the on- and off-resonance frequencies.

3. Sensitivity of sensing without detection compared to direct sensing

In the following we use a similar analysis to that used to calculate the minimum detectable gas concentration in direct detection SWIR DIAL Lidar [25]. This allows us to make direct comparison between the direct detection method and the non-linear interferometry developed here.

3.1. Sensitivity of sensing without detection

The transmittance of the gas plume can be written as

$$\mathcal{T}_{\text{on,off}} = e^{-OD_{\text{on,off}}}, \quad (9)$$

with

$$OD_{\text{on,off}} = Zn_{\text{CH}_4} \sigma_{\text{on,off}}, \quad (10)$$

where: $OD_{\text{on,off}}$ is the optical density and $\sigma_{\text{on,off}}$ is the effective absorption cross-section for on- and off-resonance MIR idler wavelength, and n_{CH_4} and Z are the number density of methane molecules and the depth of the gas plume, respectively. Thus, the differential absorption optical depth, $DAOD = OD_{\text{on}} - OD_{\text{off}}$ becomes

$$DAOD = Zn_{\text{CH}_4} (\sigma_{\text{on}} - \sigma_{\text{off}}) = \ln \left(\frac{R_{\text{off}}}{R_{\text{on}}} \right). \quad (11)$$

The quantity of scientific interest, the dry-air average volume mixing ratio of CH_4 , X_{CH_4} , is related to n_{CH_4} and number density of dry air n_{air} via $X_{\text{CH}_4} = n_{\text{CH}_4}/n_{\text{air}}$. So, Eq.(11) can be reformulated as

$$X_{\text{CH}_4} = \frac{DAOD}{Zn_{\text{air}} (\sigma_{\text{on}} - \sigma_{\text{off}})}. \quad (12)$$

For a Gaussian approximation to Poisson noise, the methane detection sensitivity of the method can be estimated by Gaussian error propagation. Propagating the error in Eq.(11), the detection precision can be written as

$$\delta X_{\text{CH}_4} = \sqrt{\left(\frac{\partial X_{\text{CH}_4}}{\partial R_{\text{on}}} \right)^2 V_{\text{on}} + \left(\frac{\partial X_{\text{CH}_4}}{\partial R_{\text{off}}} \right)^2 V_{\text{off}}} = \frac{\sqrt{SNR_{\text{on}}^{-2} + SNR_{\text{off}}^{-2}}}{Zn_{\text{air}} (\sigma_{\text{on}} - \sigma_{\text{off}})}, \quad (13)$$

where δX_{CH_4} is the minimum methane concentration that can be sensed by the apparatus. From Eq.(7), it follows that

$$\delta X_{\text{CH}_4} = \frac{1}{Zn_{\text{air}} (\sigma_{\text{on}} - \sigma_{\text{off}})} \sqrt{\frac{\hbar\omega_s}{2\eta G\alpha T_{\text{int}} P_i}}. \quad (14)$$

As we are calculating the minimum amount of methane that can be detected by the apparatus, we expect a high transmittance for both on- and off-resonance idler frequencies, so we made $\mathcal{T}_{\text{on}} = \mathcal{T}_{\text{off}} \approx 1$.

3.2. Sensitivity of direct sensing

The state-of-art methane sensors [13] exploit IPDA and DIAL techniques at SWIR, around $1.65\mu\text{m}$. For this direct sensing method, we will proceed in a similar way to calculate the sensitivity. The average of number of photons detected and its variance are

$$\langle n \rangle_{\text{on,off}} = \eta\alpha \mathcal{T}_{\text{on,off}}^2 T_{\text{int}} \frac{P_{\text{on,off}}}{\hbar\omega_{\text{on,off}}}, \quad (15)$$

where: η is the efficiency of the detector, α is the reflectivity of the lambertian background taking into account the geometric losses, T_{int} is the measurement time, $\mathcal{T}_{\text{on,off}}$ is the transmittance, $P_{\text{on,off}}$ is the power of the laser and $\hbar\omega_{\text{on,off}}$ is the energy of a photon, for on- and off-resonance wavelengths. So, the SNR for the direct sensing in the shot-noise limited scenario is

$$SNR = \sqrt{\langle n \rangle_{\text{on,off}}} = \mathcal{T}_{\text{on,off}} \sqrt{\eta\alpha T_{\text{int}} \frac{P_{\text{on,off}}}{\hbar\omega_{\text{on,off}}}}. \quad (16)$$

The $D_{AOD} = OD_{\text{on}} - OD_{\text{off}}$ for the SWIR direct sensing is

$$D_{AOD}(1.65) = Zn_{\text{CH}_4} (\sigma_{\text{on}}(1.65) - \sigma_{\text{off}}(1.65)) = \frac{1}{2} \ln \left(\frac{\langle n \rangle_{\text{off}}}{\langle n \rangle_{\text{on}}} \right), \quad (17)$$

where: $OD_{\text{on,off}}(1.65)$ is the optical density and $\sigma_{\text{on,off}}(1.65)$ is the effective absorption cross-section for on- and off-resonance SWIR laser wavelength, and n_{CH_4} and Z are the number density of methane molecules and the depth of the gas plume, respectively. For the volume mixing ratio we use X_{CH_4} the same as the one for sensing without detection, Eq.(12). It follows that the minimum amount of methane that can be detected by direct sensing is

$$\begin{aligned} \delta X_{\text{CH}_4} &= \sqrt{\left(\frac{\partial X_{\text{CH}_4}}{\partial \langle n \rangle_{\text{on}}} \right)^2 V_{\text{on}} + \left(\frac{\partial X_{\text{CH}_4}}{\partial \langle n \rangle_{\text{off}}} \right)^2 V_{\text{off}}} \\ &= \frac{1}{Zn_{\text{air}} (\sigma_{\text{on}}(1.65) - \sigma_{\text{off}}(1.65))} \sqrt{\frac{\hbar\omega}{2\eta\alpha T_{\text{int}} P}}, \end{aligned} \quad (18)$$

where we considered the same angular frequency and the same laser power for on- and off-resonance frequencies, also $\mathcal{T}_{\text{on}} = \mathcal{T}_{\text{off}} \approx 1$.

3.3. The sensitivity ratio between both methods

In this section we will compare the sensitivity between the sensing without detection and the direct sensing methods. We will analyse a scenario with a small amount of methane mixed with air in the atmosphere. We define the relative sensitivity,

$$R_S = \frac{\delta X_{\text{CH}_4} \text{ for direct measurement}}{\delta X_{\text{CH}_4} \text{ for sensing without detection}}. \quad (19)$$

This number provides us a quantitative comparison between both techniques. If we analyse a scenario that $R_S < 1$ it means that the direct sensing is more sensitive, if $R_S > 1$ the sensing without detection is more sensitive. If we make an approximating assumption that detector efficiencies, reflectivity of the backscattering surface and measurement time are equal for both wavelength scenarios then taking the ratio of Eq.(14) and Eq.(18) leads to,

$$R_S \simeq \frac{\sigma_{\text{on}}(3.22) - \sigma_{\text{off}}(3.22)}{\sigma_{\text{on}}(1.65) - \sigma_{\text{off}}(1.65)} \sqrt{G}. \quad (20)$$

The values σ can be obtained from HITRAN molecular spectroscopy database [24]. We assumed that the angular frequencies for the signal mode on the sensing without detection is the same as the one used in the direct sensing as well the laser's power, i.e. $\omega_s = \omega$ and $P_i = P$.

3.4. Simulations

Here we are interested in a typical scenario for gas sensing without detection we might expect parameters in Eq.(14) of the order

$$\begin{aligned} \eta &= 0.1, G = 10^{-8}, \alpha = 10^{-8}, T_{\text{int}} = 1\text{s}, \\ P_i &= 0.02\text{W} \text{ and } \sigma_{\text{on}} = 1.18 \times 10^{-22} \frac{\text{m}^2}{\text{molec}}. \end{aligned} \quad (21)$$

We considered a low efficiency value for the detector in the simulation as this reflects typical efficiencies in InGaAs photon counting detectors. However the high-intensity signal modes generated by SPDC can be easily detected by a higher (80%) efficiency InGaAs camera. The gain

value is approximately the one calculated for the system we have set in the lab, and using higher non-linearity or longer crystals. The value estimated for α is realistic if we consider a Lambertian background target a few tens of meters away from the apparatus. With these parameters we can reach a sensitivity of $\delta X_{CH_4} \approx 187 \text{ ppm.m}$, i. e., we can detect a methane cloud of 187 ppm concentration and one meter depth. The MIR line chosen was the one in $3.221 \mu\text{m}$ region, and we used $n_{\text{air}} = 2.53 \times 10^{25} \text{ molec.m}^{-3}$, $\sigma_{\text{off}} \approx 0$, $\lambda_s = 1.589 \mu\text{m}$.

The MIR absorption cross-section for methane in the line of $3.221 \mu\text{m}$ is around 65.1 times greater than the SWIR one at $1.65 \mu\text{m}$ ($\sigma_{on}(1.65) = 1.81 \times 10^{-24}$) [24], so the sensitivity ratio is

$$R_S \simeq 65.1 \sqrt{G}, \quad (22)$$

where we considered $\sigma_{off}(1.65) \approx 0$. Fig. 3 shows the graph of Eq.(22) in logarithmic scale. Sensitivity ratio R_S passes 2.36×10^{-4} assuming our simplistic approximations hold (equal P, α, η, T_{int} etc.).

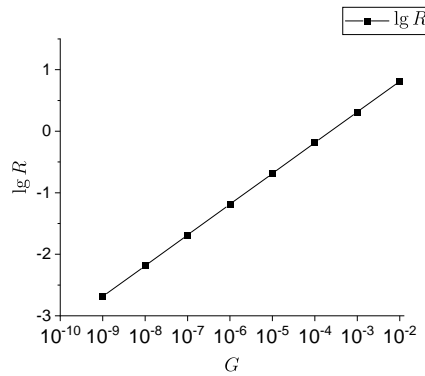


Fig. 3. Variation of the ratio of sensitivity ratio R (Eq.(22)) with G for the two different methods

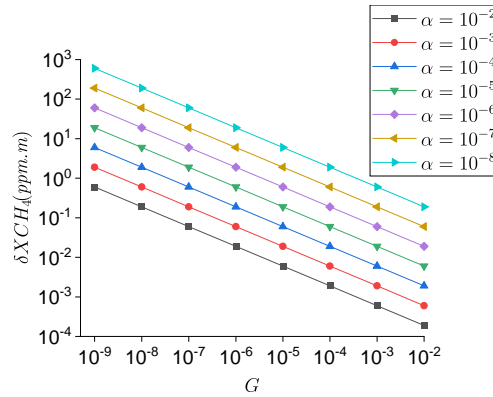


Fig. 4. The variation of δX_{CH_4} (in ppm.m) with G at different values of α shown on log-log scales.

Figure 4 shows the variation of δX_{CH_4} with G for various values of return loss α . What is significant is that for short range scenarios where a retroreflector is used and $\alpha > 10^{-2}$ then the sensitivity is better than 1 ppm.m for all values of G shown and reaches a few ppB.m at gain values $G > 10^{-4}$.

4. Conclusion

This novel gas sensing without detection method enables a new generation of high-sensitivity methane sensors. The two-colours scheme provided by sensing without detection, makes it possible to illuminate the gas with a laser in the MIR region and detect light at SWIR. This allows the gas to interact with light at a wavelength for which it exhibits a high absorption and detecting modes at shorter wavelengths where low-noise and high-efficiency detectors are available. At high gain regimes, $G > 2.36 \times 10^{-4}$, the method shows a sensitivity greater than the state-of-art IPDA and DIAL sensing techniques. This kind of nonlinear interferometer can be built in a compact fashion and light enough to be portable for field use. Analogue to the LIDAR systems, this one can provide the distance from the background scattering object by modulating the idler laser with a pseudo-random bit sequence to obtain the time of flight of the photons. High gains can be reached by using a high-efficiency crystals, high-power pump laser (or pump build up cavity) and tighter focussing into the NLC. This method can also be extended for sensing other gases as the signal and idler wavelengths can be tuned by the pump wavelength and the crystal.

Funding. This work was funded by QuantIC - the UK Quantum Technology Hub in Quantum Imaging Grant No. 8031 EP/T00097X/1 and the Innovate UK Project 106174: SPLICE.

Acknowledgments. The authors acknowledge Xiao Ai for the fruitful discussions with QLM Technology Ltd., QuantIC and SPLICE project for their support.

Disclosures. The authors declare no conflicts of interest.

Data availability. Data underlying the results presented in this paper are not publicly available at this time but may be obtained from the authors upon reasonable request.

References

1. T. F. Stocker, D. Qin, G.-K. Plattner, M. Tignor, S. K. Allen, J. Boschung, A. Nauels, Y. Xia, V. Bex and P. M. Midgley, eds., "Climate Change 2013: The Physical Science Basis. Contribution of Working Group I to the Fifth Assessment Report of the Intergovernmental Panel on Climate Change," (Cambridge University Press, Cambridge, United Kingdom and New York, NY, USA, 2013).
2. M. Etminan, G. Myhre, E. J. Highwood, K. P. Shine, "Radiative forcing of carbon dioxide, methane, and nitrous oxide: A significant revision of the methane radiative forcing," *Geophys. Res. Lett.* **43**, 12614–12623 (2016).
3. T. Blunier, J. A. Chappellaz, J. Schwander, J.-M. Barnola, T. Desperts, B. Stauffer, D. Rayna, "Atmospheric methane, record from a Greenland ice core over 1000 year," *Geophys. Res. Lett.* **20**, 2219–2222 (1993).
4. D. Etheridge, L. Steele, R. Francey, R. Langenfelds, "Atmospheric methane between 1000 A.D. and present: evidence of anthropogenic emissions and climatic variability," *Journal Geophys. Res.* **103**, 15979–15993 (1998).
5. D. J. Wuebbles, K. Hayhoe, "Atmospheric methane and global change," *Earth-Science Rev.* **57**, 177–210 (2002).
6. P. Bousquet, P. Ciais, J. B. Miller, E. J. Dlugokencky, D. A. Hauglustaine, C. Prigent, G. R. Van der Werf, P. Peylin, E.-G. Brunke, C. Carouge, R. L. Langenfelds, J. Lathière, F. Papa, M. Ramonet, M. Schmidt, L. P. Steele, S. C. Tyler, J. White, "Contribution of anthropogenic and natural sources to atmospheric methane variability," *Nature* **443**, 439–443 (2006).
7. D. Shindell, J. C. I. Kylenstierna, E. Vignati, R. van Dingenen, M. Amann, Z. Klimont, S. C. Anenberg, N. Muller, G. Janssens-Maenhout, F. Raes, J. Schwartz, G. Faluvegi, L. Pozzoli, K. Kupiainen, L. Höglund-Isaksson, L. Emberson, D. Streets, V. Ramanathan, K. Hicks, N. T. Kim Oanh, G. Milly, M. Williams, V. Demkine, D. Fowler, "Simultaneously mitigating near-term climate change and improving human health and food security," *Science* **335**, 6065 183–189 (2012).
8. A. Butz, S. Guerlet, O. Hasekamp, D. Schepers, A. Galli, I. Aben, C. Frankenberg, J.-M. Hartmann, H. Tran, A. Kuze, G. Keppel-Aleks, G. Toon, D. Wunch, P. Wennberg, N. Deutscher, D. Griffith, R. Macatangay, J. Messerschmidt, J. Notholt, T. Warneke, "Toward accurate CO₂ and CH₄ observations from GOSAT," *Geophys. Res. Lett.* **38**, L14812 (2011).
9. D. J. Jacob, A. J. Turner, J. D. Maasakkers, J. Sheng, K. Sun, X. Liu, K. Chance, I. Aben, J. McKeever, C. Frankenberg, "Satellite observations of atmospheric methane and their value for quantifying methane emissions," *Atmospheric Chem. Phys.* **16**, 14371–14396 (2016).
10. L. M. Golston, L. Tao, C. Brosy, K. Schäfer, B. Wolf, J. McSpiritt, B. Buchholz, D. R. Caulton, D. Pan, M. A. Zondlo, D. Yoel, H. Kunstmann, M. McGregor, "Lightweight mid-infrared methane sensor for unmanned aerial systems," *Appl. Phys. B* **123**, 170 (2017).
11. K. C. Cossel, E. M. Waxman, F. R. Giorgetta, M. Cermak, I. R. Coddington, D. Hesselius, S. Ruben, W. C. Swann, Gar-Wing Truong, G. B. Rieker, N. R. Newbury, "Open-path dual-comb spectroscopy to an airborne retroreflector," *Optica* **4**, 724–728 (2017).

12. N. Cezard, S. Le Mehaute, J. Le Gouët, M. Valla, D. Goular, D. Fleury, C. Planchat, A. Dolfi-Bouteyre, "Performance assessment of a coherent DIAL-Doppler fiber Lidar at 1645 nm for remote sensing of methane and wind," *Opt. Express* **28**, 22345–22357 (2020).
13. J. Titchener, D. Millington-Smith, C. Goldsack, G. Harrison, A. Dunning, X. Ai, M. Reed, "Single photon Lidar gas imagers for practical and widespread continuous methane monitoring," *Appl. Energy* **306**, Part B 118086 (2022).
14. G. B. Lemos, V. Borish, G. D. Cole, S. Ramelow, R. Lapkiewicz, A. Zeilinger, "Quantum imaging with undetected photons," *Nature* **512**, 409–412 (2014).
15. A. C. Cardoso, L. P. Berrueto, D. F. Ávila, G. B. Lemos, W. M. Pimenta, C. H. Monken, P. L. Saldanha, S. Pádua, "Classical imaging with undetected light," *Phys. Rev. A* **97**, 033827 (2018).
16. S. K. Lee, T. H. Yoon, M. Cho, "Molecular Rovibrational Spectroscopy with Undetected Photons via Single-Photon Interferometry," *Phys. Rev. Appl.* **14**, 014045 (2020).
17. I. Kviatkovsky, H. M. Chrzanowski, E. G. Avery, H. Bartolomaeus, S. Ramelow, "Microscopy with undetected photons in the mid-infrared," *Sci. Adv.* **6**, 42 (2020).
18. I. Kviatkovsky, H. M. Chrzanowski, S. Ramelow, "Mid-infrared microscopy via position correlations of undetected photons," *Opt. Express* **30**, 5916-5925 (2022).
19. S. Töpfer, M. G. Basset, J. Fuenzalida, F. Steinlechner, J. P. Torres, M. Gräfe, "Quantum holography with undetected light," *Sci. Adv.* **8**, 2 (2022).
20. G. J. Machado, G. Frascella, J. P. Torres, M. V. Chekhova, "Optical coherence tomography with a nonlinear interferometer in the high parametric gain regime," *Appl. Phys. Lett.* **117**, 094002 (2020).
21. A. Vanselow, P. Kaufmann, I. Zorin, B. Heise, H. M. Chrzanowski, S. Ramelow, "Frequency-domain optical coherence tomography with undetected mid-infrared photons," *Optica* **7**, 1729-1736 (2020).
22. M. Kutas, B. Haase, P. Bickert, F. Rixinger, D. Molter, G. von Freymann, "Terahertz quantum sensing," *Sci. Adv.* **6**, 11 (2020).
23. X. Sun, J. B. Abshire, "Signal to noise ratios of pulsed and sinewave modulated direct detection lidar for IPDA measurements," in *Conference on Lasers and Electro-Optics (CLEO) - Laser Science to Photonic Applications* (2011), pp. 1-2.
24. L. Rothman et al., "The HITRAN 2012 molecular spectroscopic database," *J. Quant. Spectrosc. Radiat. Transf.* **130** 4-50 (2013).
25. M. Quatrevallet, X. Ai, A. Perez-Serrano, P. Adamiec, J. Barbero, A. Fix, J. M. G. Tijero, I. Esquivias, J. G. Rarity, G. Ehret, Atmospheric CO₂ Sensing with a Random Modulation Continuous Wave Integrated Path Differential Absorption Lidar, *IEEE Journal of Selected Topics in Quantum Electronics* 23 (2), 157-167 (2017).